Nanopackaging:
Nanotechnologies & Electronics Packaging
Part A Nanoparticles

James E. Morris
Department of Electrical & Computer Engineering,
Portland State University, Portland, Oregon, USA
j.e.morris@ieee.org

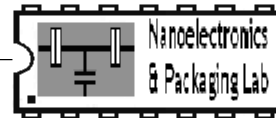

Nanopackaging

- Nanotechnologies in Microelectronics Packaging
  - Nanoparticles
  - Carbon nanotubes
  - Nanoparticles & CNTs in ECAs
  - Nanowires, nanospring contacts
  - Modeling: Molecular Dynamics to Effective Medium
- Nanoelectronics Packaging
- Health & environment
  - CNTs in the body
  - Nano-Ag toxicity to bacteria
- "Nanopackaging: Nanotechnologies in Electronics Packaging," J.E. Morris (editor) Springer (August 2008)

4/21/2009

Copper Nano-Twins (Zhang et al, Appl Phys Lett/Nanotechweb, 2008)

Cu Nano-twins increase conductivity and mechanical strength. Nano-grains increase strength; twins reduce high angle grain boundary scattering and block single dislocations

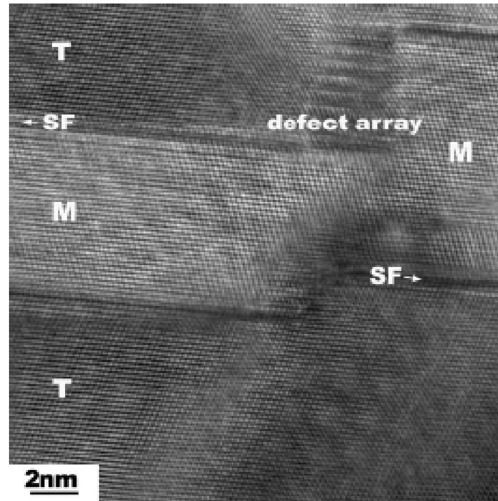

Nanoparticles

- Preparation
- General properties
- Melting point depression
- Charging effects
- Dielectrics
- Interconnects
- Miscellaneous applications
- Solder
- Nanoelectronics: Nanoparticle arrays, SETs, & charging re-visited

Ag nanoparticle synthesis

[←Jiang/Moon/Wong APM'05]
[Pothukuchi/Li/Wong ECTC'04]

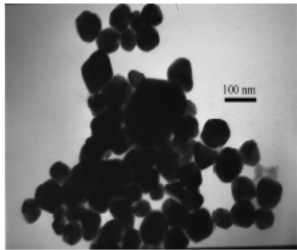

Fig. 4 TEM micrographs for copper and silver alloy nanoparticles under the reaction of 3ml PVP and 3ml copper acetate for 20 mins, then add 3 ml silver nitrate and react for another 5 mins.

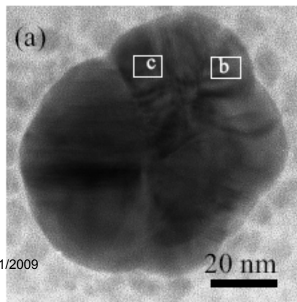

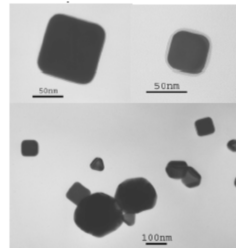

Figure.1 Silver nanocubes as obtained by the procedure detailed.

Nanoparticle Fabrication

Breakdown method

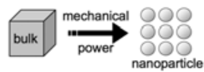

Buildup method

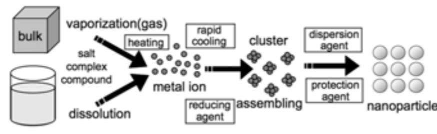

gas condensation

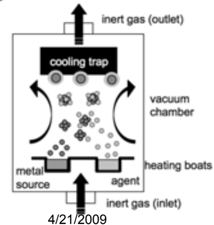

atomization

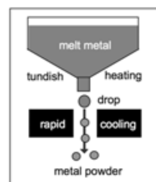

Liquid-solid Sonochemical Reaction: Metal oxide particles in EtOH

(Hayashi et al)

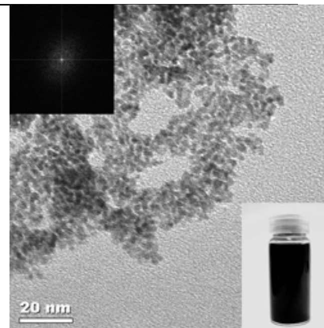

Surface treatments to avoid agglomeration

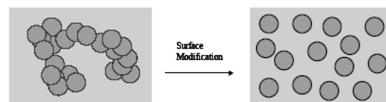

Figure 1. Scheme of surface modification for nano-size filler

Sun & Wong, ECTC'04

AFM Fabrication

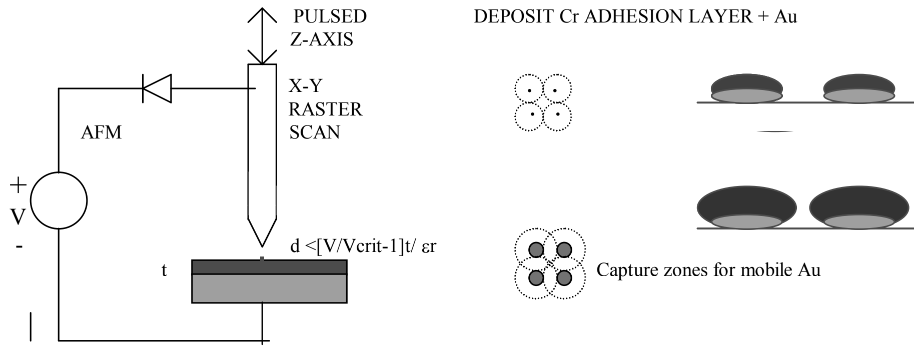

Nanoparticle Properties

Electron transport mechanisms at small dimensions include ballistic transport, severe mean free path restrictions in very small nanoparticles, various forms of electron tunneling, electron hopping mechanisms, and more.

Other physical property changes include:

- Melting point depression, i.e. the reduction of metal nanoparticle melting points at small sizes, although this is unlikely to be a factor in packaging applications with even 10% reductions typically requiring dimensions under 5nm
- Sintering by surface self-diffusion, which is thermally activated, with net diffusion away from convex surfaces of high curvature
- The Coulomb blockade effect, which requires an external field or thermal source of electrostatic energy to charge an individual nanoparticle, and is the basis of single-electron transistor operation
- Theoretical maximum mechanical strengths in single grain material structures
- Unique optical scattering properties by nanoparticles one to two orders smaller than the wavelength of visible light
- The enhanced chemical activities of nanoparticles, which make them effective as catalysts, and other effects of the high surface-to-volume ratio

Nanoparticle Properties (High surface/volume ratio→catalysts, etc)

Nanoparticles → single grain, no defects (Mallik)

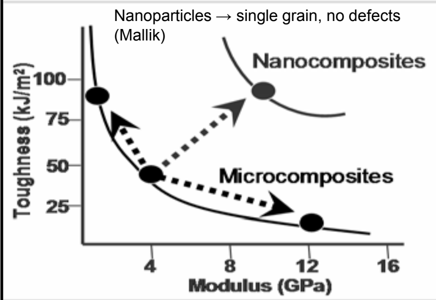

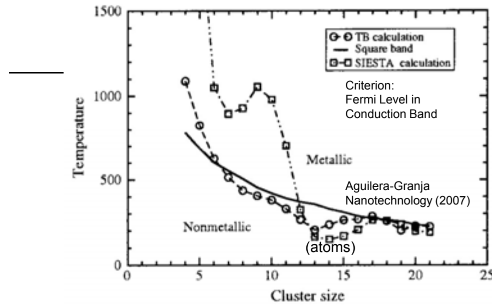

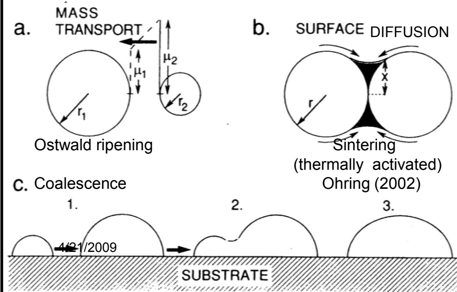

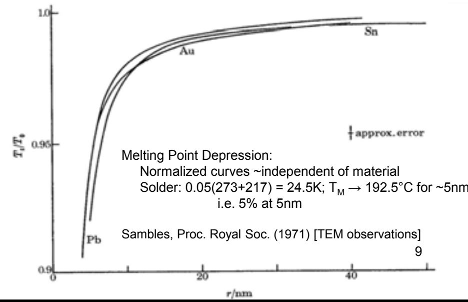

Melting Point Depression:
Normalized curves ~independent of material
Solder: 0.05(273+217) = 24.5K; T_M → 192.5°C for ~5nm
i.e. 5% at 5nm

Sambles, Proc. Royal Soc. (1971) [TEM observations]

Melting point depression

[Sambles, Proc Roy Soc]

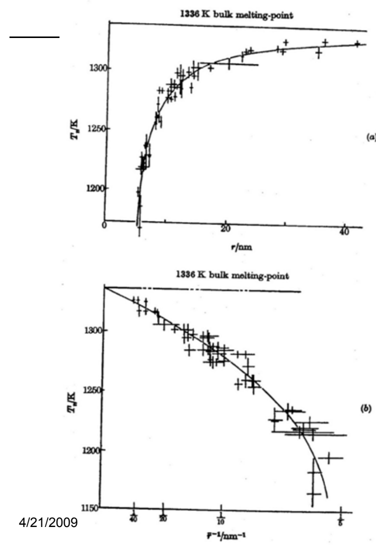

5. (a) Variation of melting temperature with gold particle radius, and (b) variation of reciprocal radius with melting temperature for gold particles.

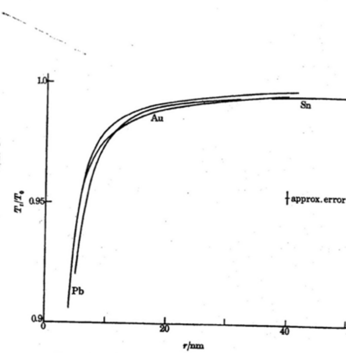

Figure 7. Variation of reduced melting temperature with radius for gold (Sambles), lead (Coombes) and tin (Wronski).

MP Depression in SnAg Nanoparticles

(Hongjin Jiang et al, ECTC'07) [found by DSC]

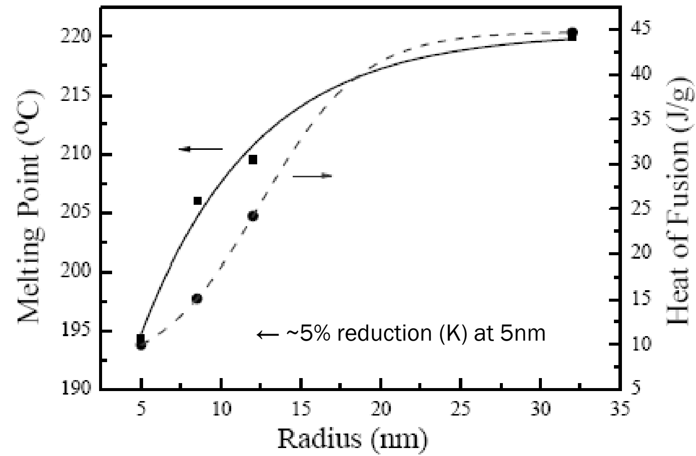

Melting Point Depression in No-Pb Solder Nanoparticles (Liu, Andersson, Gao, & Zhai, EPTC 2008)

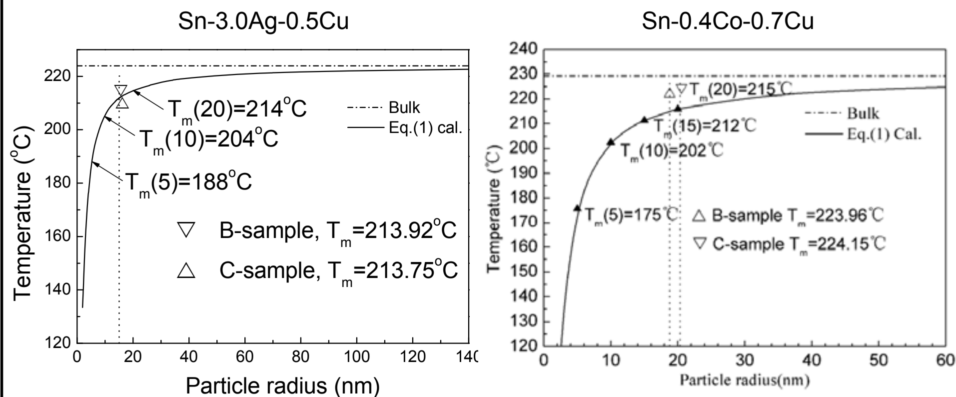

Nanoparticle Charging:
the Coulomb Block (Morris)

Spherical nanoparticles, radius r, separation s
Electrostatic charging energy:

$$\Delta E = \frac{q^2}{4\pi\varepsilon r} \rightarrow \frac{q^2}{4\pi\varepsilon}\left[\frac{1}{r} - \frac{1}{r+s}\right]$$

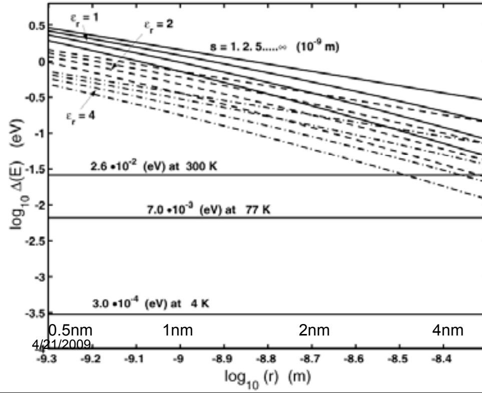

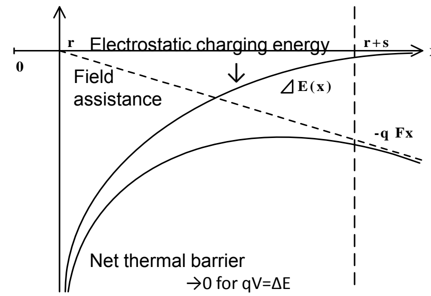

Embedded Cermet Resistors: $Cr_x(SiO)_{1-x}$ & $(Cr_xSi_{1-x})_{1-y}N_y$

Electromicrographs of $(Cr_xSi_{1-x})_{1-y}N_y$ films (a) x=0.4, y=0, (b) x=4, y=0.1.

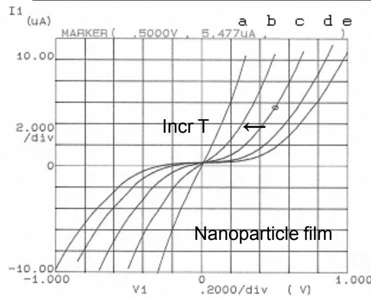

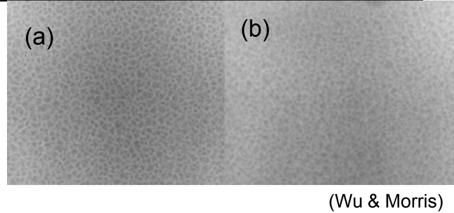

(Wu & Morris)

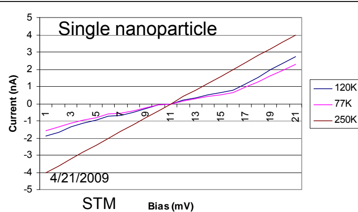

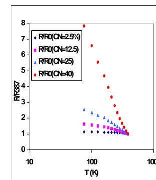

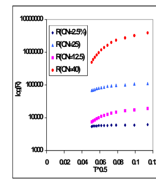

[80]:[20] [SiO]:[Cr] R(T) +ve/-ve TCRs

Balance $TCR_{\Delta E}$ <0 and TCR_{metal} >0

(Wu & Morris)

I-V characteristics of $Cr_x(SiO)_{1-x}$

Electrical characteristics typical of Coulomb Blockade devices

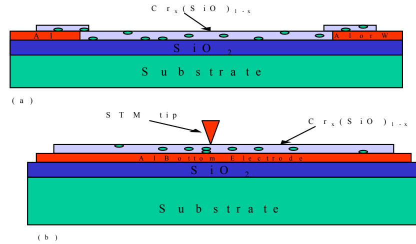

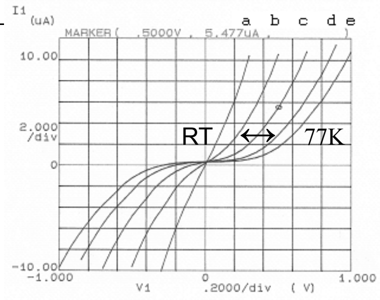

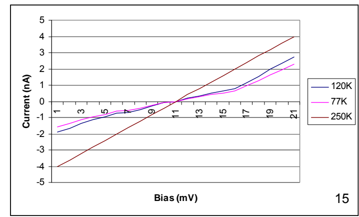

Coulomb effects "wash out" at room temperature (thermal charging)

Embedded Capacitors: High-*k* Composites

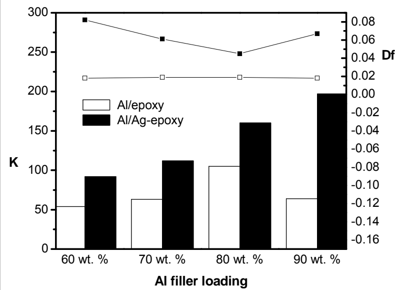

(Lu & Wong)

Organic surface layer modification: Insulating layer prevents metallic contacts

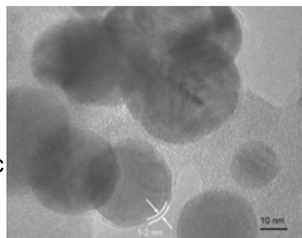

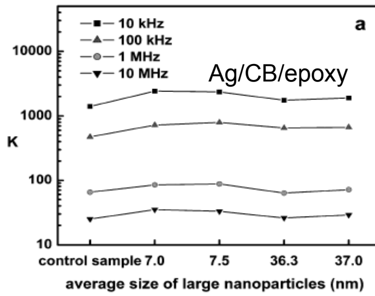

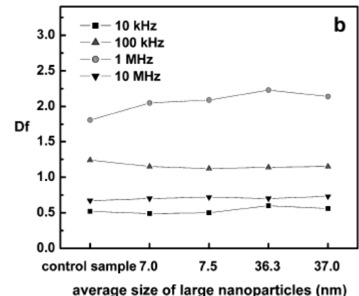

Note: $BaTiO_3$ nanoparticles

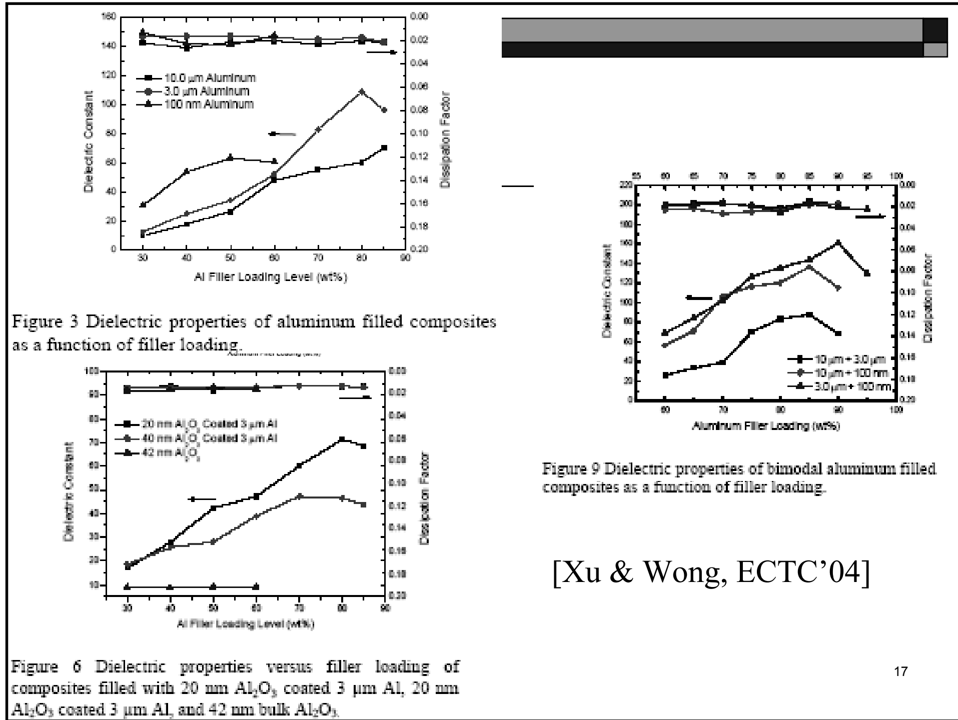
Figure 3 Dielectric properties of aluminum filled composites as a function of filler loading.
Figure 6 Dielectric properties versus filler loading of composites filled with 20 nm Al_2O_3 coated 3 μm Al, 20 nm Al_2O_3 coated 3 μm Al, and 42 nm bulk Al_2O_3.
Figure 9 Dielectric properties of bimodal aluminum filled composites as a function of filler loading.
[Xu & Wong, ECTC'04]
17

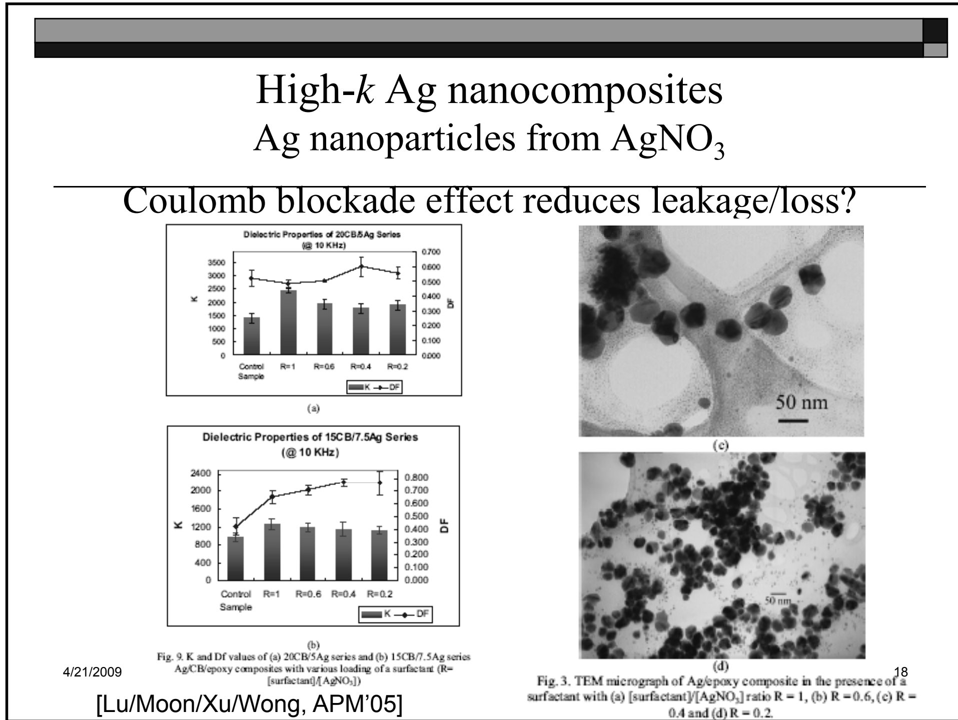
High-*k* Ag nanocomposites
Ag nanoparticles from $AgNO_3$
Coulomb blockade effect reduces leakage/loss?
Dielectric Properties of 15CB/7.5Ag Series
(@ 10 KHz)
Fig. 9. K and Df values of (a) 20CB/5Ag series and (b) 15CB/7.5Ag series Ag/CB/epoxy composites with various loading of a surfactant (R= [surfactant]/[$AgNO_3$])
Fig. 3. TEM micrograph of Ag/epoxy composite in the presence of a surfactant with (a) [surfactant]/[$AgNO_3$] ratio R = 1, (b) R = 0.6, (c) R = 0.4 and (d) R = 0.2.
50 nm
4/21/2009
18
[Lu/Moon/Xu/Wong, APM'05]

High-*k* $BaTiO_3$/polymer nanocomposite gate dielectric reduces V_T for OFETs [Rasul et al, ECTC'06]

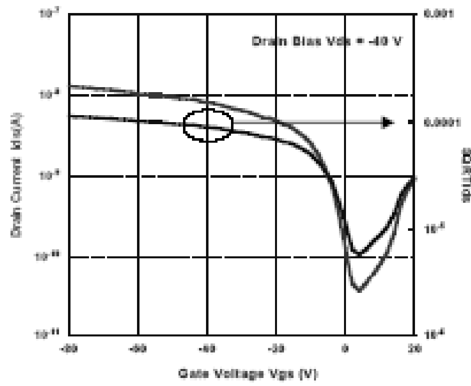

Figure 6. Plot of sqrt. drain current $(I_D)^{1/2}$ vs. gate voltage (V_G) and drain current (I_D) vs. gate voltage (V_G) (transfer) characteristics, V_D = -40 V.

TCC control of nanocomposite capacitors: High-*k* $BaTiO_3$- & low-*k* BCB

[Abothu et al, ECTC'06]

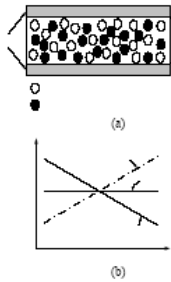

Fig. 1 (a) Schematic of nanocomposite capacitor made of positive and negative TCC fillers and (b) its TCC behavior to be expected.

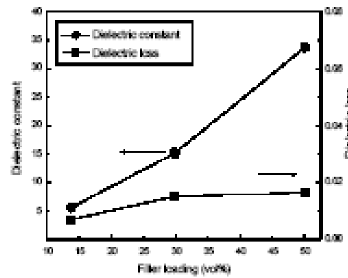

Fig. 3 Room temperature dielectric properties of BT-BCB nanocomposites (at 100 KHz) with ceramic filler loading.

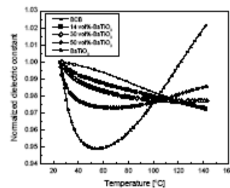

Fig. 5 Normalized dielectric constants of nanocomposites with different ceramic filler loading, pure BT and pure BCB as a function of temperature.

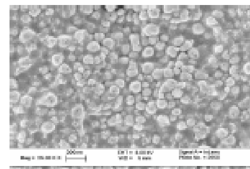

Fig. 2 SEM micrograph of BT-BCB nanocomposite with 50 vol% ceramic filler loading.

(Herzer/Jha et al)

Embedded Inductance/Transformers

High μ_r & low H_c for small grains <10nm

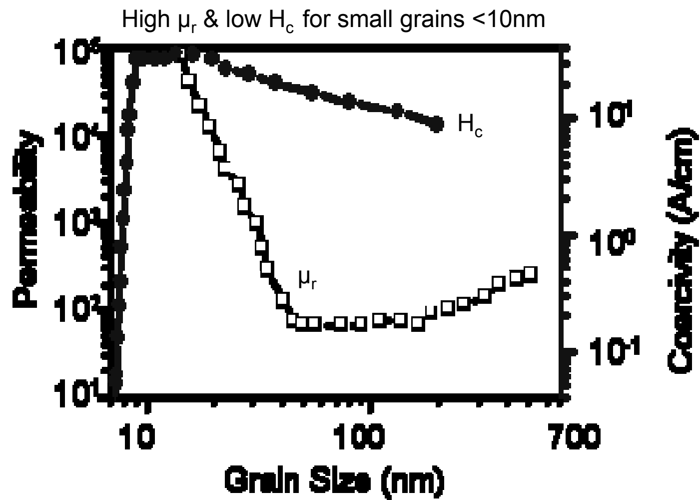

Inkjet nanoparticle interconnect printing

[Kolbe et al, ECTC'05]

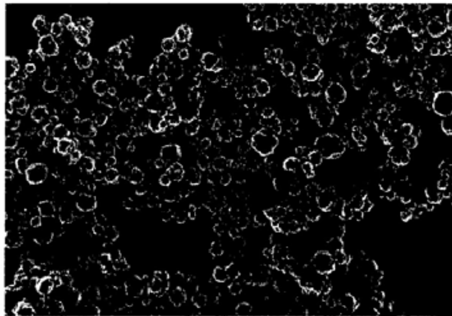

Figure 1 Scanning electron micrograph of the silver powder

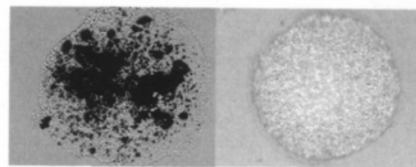

Figure 3 Micrograph of a printed droplet with agglomerated filler particles (left) and with a homogeneous filler particle distribution (right)

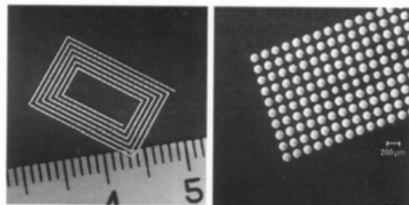

Figure 4 Ink jet printed antenna and dots of adhesive

Printed Nanoparticle Interconnect Deposition

(Felba & Schaeffer)
e.g. on flex

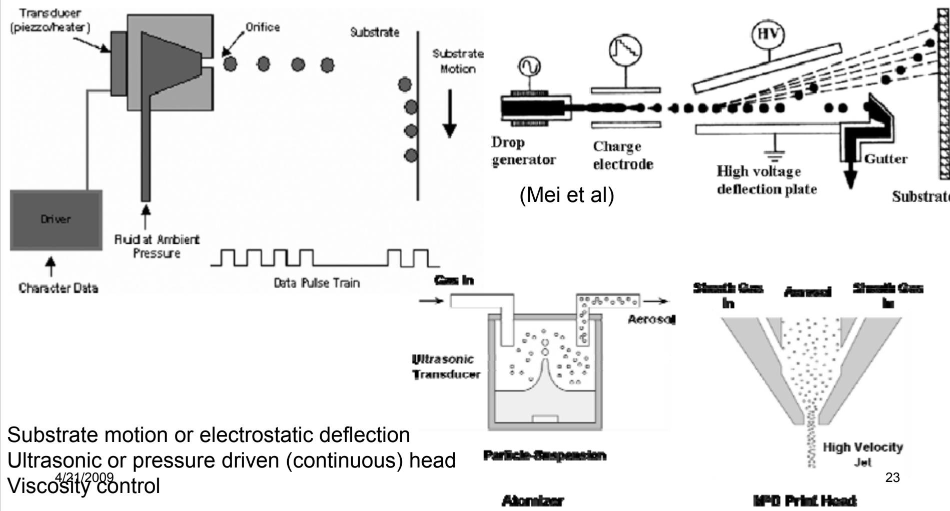

Substrate motion or electrostatic deflection
Ultrasonic or pressure driven (continuous) head
Viscosity control

Deposited Interconnect Material

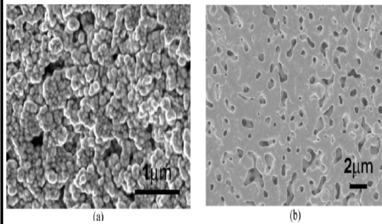

Nanoscale Ag on Si, before and after sintering at 280° (Bai et al)

Ag nanoparticle paste : Initially, and after dipping in methanol for 180s, 600s, 3600s (Wakuda et al)

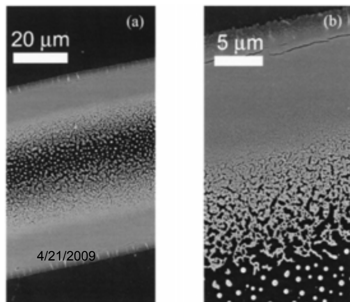

Au line cured by 300mW laser (Bieri et al)

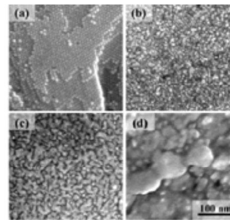

(Felba & Schaeffer)

Nano-Silica Flip-Chip Underfill

CTE/modulus reduction with less settling

(Lall et al)

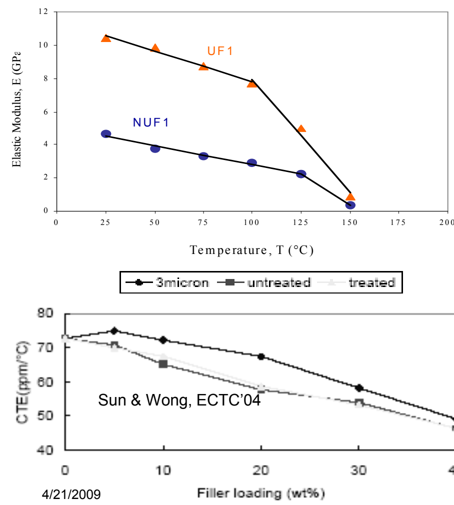

Untreated: Agglomerated

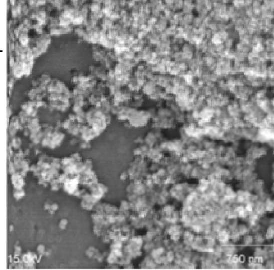

Silane treated:

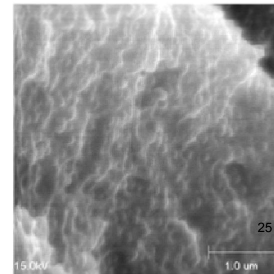

Figure 6 CTE of silica filled composite underfills

Low-*k* Si nano-composite:

SiH_4/organic PECVD: Deep UV *n, k* control

[Kubacki, ECTC'06]

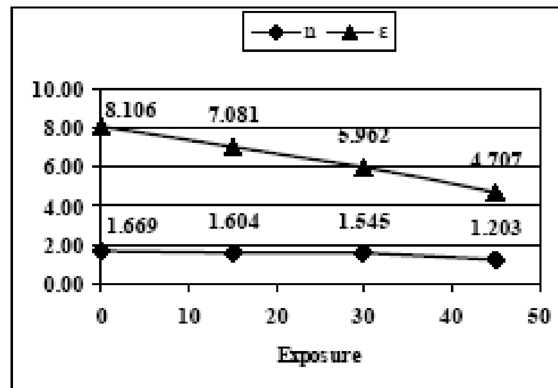

Fig. 2. Index of refraction *n*, and dielectric constant *ε* for Sample 2.

Thermal conductivity: Al_2O_3 nanoparticles

[Fan/Su/Qu/Wong ECTC'04]

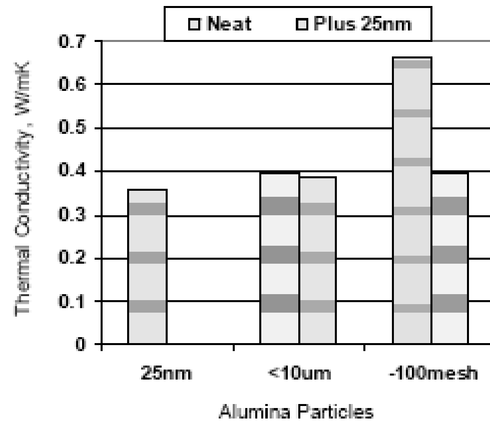

Figure 10. Thermal conductivities of composite samples with different particle sizes and their combinations

Photodefinable (resist) stress relief layer (with silica nanoparticles)

[Sun/Zhang/Wong ECTC'05]

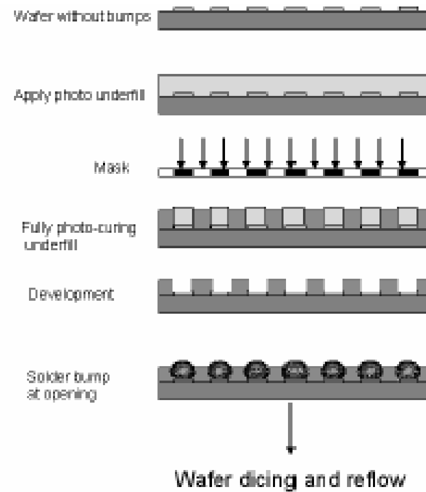

Figure 1 Proposed wafer process with novel photo-definable nanocomposite

Metal Nanoparticles added to SnAg Solder:

Intermetallic Compound (IMC) Growth (Amagai)

One solder reflow

Four solder reflows

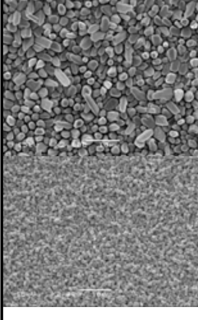

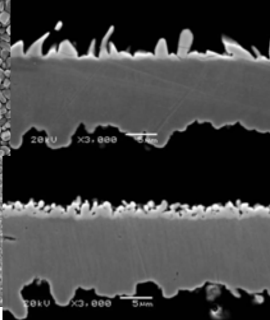

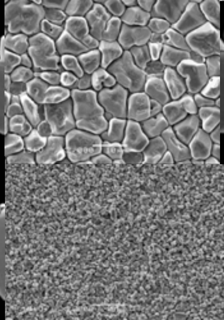

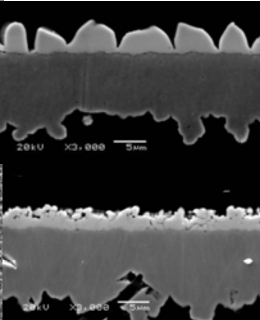

Top:

Sn3.0Ag solder IMC growth

Most no effect.

Periodic Table

Na Mg Al Si P S Cl Ar

1 2 3 4 5 6 7 8 9 10 11 12 13 14 15 16 17 18

K Ca Sc Ti V Cr Mn Fe Co Ni Cu Zn Ga Ge As Se Br Kr

Rb Sr Y Zr Nb Mo Tc Ru Rh Pd Ag Cd In Sn Sb Te I Xe

Cs Ba * Hf Ta W Re Os Ir Pt Au Hg Tl Pb Bi Po At Rn

Bottom:

Sn3.0Ag0.03Ni limits IMC growth.

Also Co, Pt

Summary of added Metallic nanoparticle effects

(Amagai)

Nano Particle	Wt%	IMC comparison with Sn3.0Ag after 4 time reflow processes		IMC change from 1 time to 4 time reflow processes	
		Grain Size	Thickness	Grain Size	Thickness
Ni	0.01	Small	Low	Not large	Not large
	0.03	Small	Low	Small	Small
	0.05	Small	Low	Small	Small
Cu	0.1	Same	Same	Large	Large
	0.3	Same	Same	Large	Large
	0.5	Same	Same	Large	Large
	0.7	Same	Same	Large	Large
	1	Same	Same	Large	Large
Co	0.01	Small	Low	Not large	Not large
	0.03	Small	Low	Small	Small
In	0.1	Same	Same	Large	Large
	0.2	Same	Same	Large	Large
	0.3	Same	Same	Large	Large
Sb	0.1	Same	Same	Large	Large
	0.3	Same	Same	Large	Large
	0.5	Same	Same	Large	Large
Zn	0.05	Same	Same	Large	Large
	0.1	Same	Same	Large	Large
P	0.03	Same	Same	Large	Large
Au	0.1	Same	Same	Large	Large
Ge	0.05	Same	Same	Large	Large
Pt	0.05	Small	Low	Small	Small
Al	0.05	Same	Same	Large	Large

Drop tests for nanoparticles in SAC solder: Co, Ni, Pt inhibit IMC formation

[Amagai, ECTC'06]

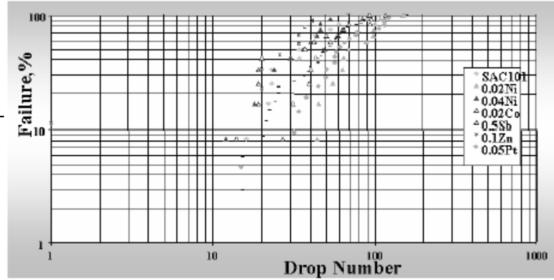

Figure 37 A weibull plot of drop test failure for 0.02Ni, 0.04Ni, 0.02Co, 0.5Sb, 0.1Zn, or 0.05Pt including in Sn1.0Ag0.01Cu and a reference solder (Sn1.0Ag0.01Cu , SAC101) before 100°C thermal aging (100 hours) .

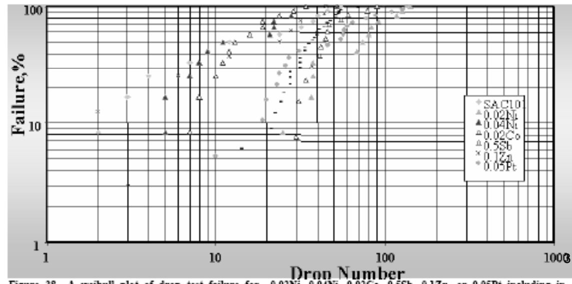

Figure 38 A weibull plot of drop test failure for 0.02Ni, 0.04Ni, 0.02Co, 0.5Sb, 0.1Zn, or 0.05Pt including in Sn1.0Ag0.01Cu and a reference solder (Sn1.0Ag0.01Cu , SAC101) after 100°C thermal aging (100 hours) .